# Evolution of a novel left-right asymmetry involving tissue remodelling and MyoID.

Bénédicte M. Lefèvre[1,2], Marine Delvigne[1], Josué Vidal[1], Virginie Courtier-Orgogozo[1*¶], and Michael Lang[1,3*¶]

[1]Université Paris Cité, CNRS, Institut Jacques Monod, F-75013 Paris, France.

[2]current address: Team "Stem Cells and Tissue Homeostasis", Institut Curie, CNRS, UMR3215, INSERM U934, PSL Research University, 26 rue d'Ulm, 75248 Paris Cedex 05

[3]current address: Laboratoire Évolution, Génomes, Comportement et Écologie, CNRS, IRD, Université Paris-Saclay – Institut Diversité, Ecologie et Evolution du Vivant (IDEEV), 91190 Gif-sur-Yvette, France

[¶]co-last authors.

*co-corresponding authors:

Michael Lang, **Email:** michael.lang@universite-paris-saclay.fr,

Virginie Courtier-Orgogozo, **Email:** virginie.courtier@normalesup.org

## Abstract

Left-right asymmetries recurrently evolve in animals but the underlying developmental mechanisms are unknown. In most *Drosophila* species, the male genitalia is symmetric and undergoes a clockwise 360° rotation during development. In *D. melanogaster*, this tissue remodeling process is directed by class I myosins: in MyoID mutants the rotation is reversed and the genitalia remains symmetric. Males of *Drosophila pachea* have evolved unique left-right asymmetric genital organs and a characteristic right-sided copulation posture in the past 3-6 million years. To test if these asymmetries in morphology and behavior evolved via the recruitment of pre-existing directional cues controlled by MyoID, we used CRISPR to knockout MyoID in *D. pachea*. Strikingly, mutant males undergo a reverse genitalia rotation and develop mirror-image asymmetric genitalia, indicating that MyoID controls both the direction of genitalia rotation direction and morphological asymmetry. Although genital asymmetry is reversed, MyoID mutants still adopt a wild-type right-sided copulation posture. Our results show that MyoID and its asymmetry guidance role were recruited for the evolution of a novel left-right asymmetry in *D. pachea* and that lateralized copulation behavior is determined by other mechanisms. The evolution of a new left-right organ size asymmetry in *D. pachea* involved recruitment of existing directional cues.

# Introduction

While the outer bodyparts of most bilaterian animals are left-right symmetric, some organs display left-right asymmetries in position, shape or size (Hamada and Tam, 2020). The generation of asymmetric organs during development starts with an initial symmetry-breaking step, which can involve several mechanisms: motile cilia and directional fluid flow, orientation of the cell division plane and distribution of molecules within cells (Hamada and Tam, 2020; Lai et al., 2022). How over the course of evolution initially symmetrical organs become asymmetric remains elusive. Males of the fruitfly *Drosophila pachea* have an asymmetric phallus with a right-sided opening for sperm release (gonopore) and a pair of asymmetric external genital lobes, with the left lobe being 1.5 times longer than the right lobe (Fig 1 A,B) (Acurio et al., 2019; Lang and Orgogozo, 2012; Pitnick and Heed, 1994). The lobes are considered an evolutionary novelty since they are not present in the three closely related sister species (Lang et al., 2014). *D. pachea* flies also mate in a right-sided posture with the male being shifted about 6-8° towards the right side of the female (Acurio et al., 2019; Lang and Orgogozo, 2012; Rhebergen et al., 2016). The lobes function as a grasping device and stabilize the copulatory complex at the onset and during copulation (Lefèvre et al., 2021; Rhebergen et al., 2016). Asymmetric male genitalia and right-sided mating behavior have probably repeatedly evolved in *D. pachea* and closely related species within the past 3-6 Ma (Acurio et al., 2019; Lang et al., 2014). Genital asymmetry has been hypothesized to evolve in response to changes in mating position (Huber, 2010). Alternatively, asymmetric genitalia may provoke lateralized mating behavior since the asymmetric parts mediate the coupling of the female and male abdomen during copulation. Overall, the reciprocal effects of behavioral changes and evolution of morphology cannot be generalized and require case-specific assessments, in particular with respect to reproduction (Huber, 2010).

During development, the male genitalia of a wide range of shizophoran flies undergo a 360° clockwise rotation (Feuerborn, 1922; Suzanne et al., 2010). In *D. melanogaster*, the direction of this rotation is driven by the myosin MyoID,

encoded by the gene *myo31DF* (Spéder et al., 2006), for simplicity here referred to as *myoID*. Loss of function of *myoID* in *D. melanogaster* leads to a counter-clockwise 360° genitalia rotation direction, due to the function of another counter-acting myosin, MyoIC (Petzoldt et al., 2012; Spéder et al., 2006; Suzanne et al., 2010). MyoID also controls the chirality of other organs, such as the hindgut and testes (Benitez et al., 2010; González-Morales et al., 2015; Hatori et al., 2014; Hozumi et al., 2006; Okumura et al., 2015; Spéder et al., 2006; Taniguchi et al., 2011, 2007). Furthermore, MyoID appears to be a conserved key factor among different mechanisms to establish left-right asymmetry in vertebrates and invertebrates (Juan et al., 2018; Tingler et al., 2018), through interaction with adherens junctions (Petzoldt et al., 2012; Taniguchi et al., 2011), the actin cytoskeleton (Chougule et al., 2020; Lebreton et al., 2018; Petzoldt et al., 2012), planar cell polarity pathway members (González-Morales et al., 2015; Juan et al., 2018; Lai et al., 2022) and Jun kinase pathway regulated apoptosis (Benitez et al., 2010; Macias et al., 2004; Rousset et al., 2010; Taniguchi et al., 2007). Ectopically expressed, MyoID and MyoIC are sufficient to induce *de novo* directional twisting at the cell, organ, or body scale in *D. melanogaster* (Lebreton et al., 2018). However, the evolutionary transitions to *novel* left-right size asymmetries remain to be uncovered at the molecular, cellular and tissue scale.

# Results & Discussion

We wondered if MyoID is involved in the establishment of left-right asymmetry in *D. pachea* male genitalia (Figure 1 A,B). To test this, we generated a mutation in the coding sequence of the *D. pachea myoID* using CRISPR/Cas9 mediated gene editing (Bassett et al., 2013; Jinek et al., 2012) (*myoID*$^{mut}$ allele, supplementary Figure 1). The induced mutation caused a frameshift in the seventh coding exon, leading to a premature stop codon (Materials and Methods). In homozygous *myoID*$^{mut/mut}$ males, the length ratio of left and right genital lobes was reversed with a longer right lobe and a shorter left lobe in most (81/82) dissected individuals (supplementary datafile 1, Figure 1C). Furthermore, the phallus asymmetry was reversed in *myoID*$^{mut/mut}$ males with the gonopore located at the left tip of the phallus (29/29 dissected genitalia), compared to

heterozygous *myoID*$^{wt/mut}$ and *myoID*$^{wt/wt}$ males, where the gonopore was located consistently on the right side (8/8 and 13/13 dissected genitalia, respectively; supplementary Figure 2). The locus *myoID* is autosomal (supplementary Figure 1) and the mutation appears to be recessive since *myoID*$^{wt/mut}$ males did not have visible alterations of male genitalia morphology compared to *myoID*$^{wt/wt}$ males (Figure 1B). Apart from phallus and lobe morphology, homozygous mutant males revealed a genitalia rotation phenotype, with varying orientations of the male genitalia in adults, with respect to the antero-posterior midline (Figure 1 A,D). In wild-type *D. pachea*, male surstili (claspers) and genital lobes are pointing towards the anterior ventral body (Figure 1A), while *myoID*$^{mut/mut}$ males revealed variable orientations of genitalia, which varied among individuals between 0 and 270° (Figure 1D). This latter orientation phenotype was similar to previous observations in *D. melanogaster myoID* mutants (Spéder et al., 2006). Our data shows that MyoID is essential to determine left-right identity in *D. pachea* male genitalia, including external genital lobes and the male phallus. This function might be mediated through its role in determining the direction of male genitalia rotation. In one *myoID*$^{mut/mut}$ males, genital lobe asymmetry was not reversed although genitalia were mis-oriented and in one individual lobes were strongly bent. However, it was unclear if their genitalia rotated clockwise or counter-clockwise during development. These mutants may have had remnant activity and expression of the *myoID*$^{mut}$ allele, leading to a partial rotation in clockwise direction. Alternatively, other unidentified environmental or genetic factors may also contribute to the determination of genital asymmetry in *D. pachea* and were variable in our experiment.


4

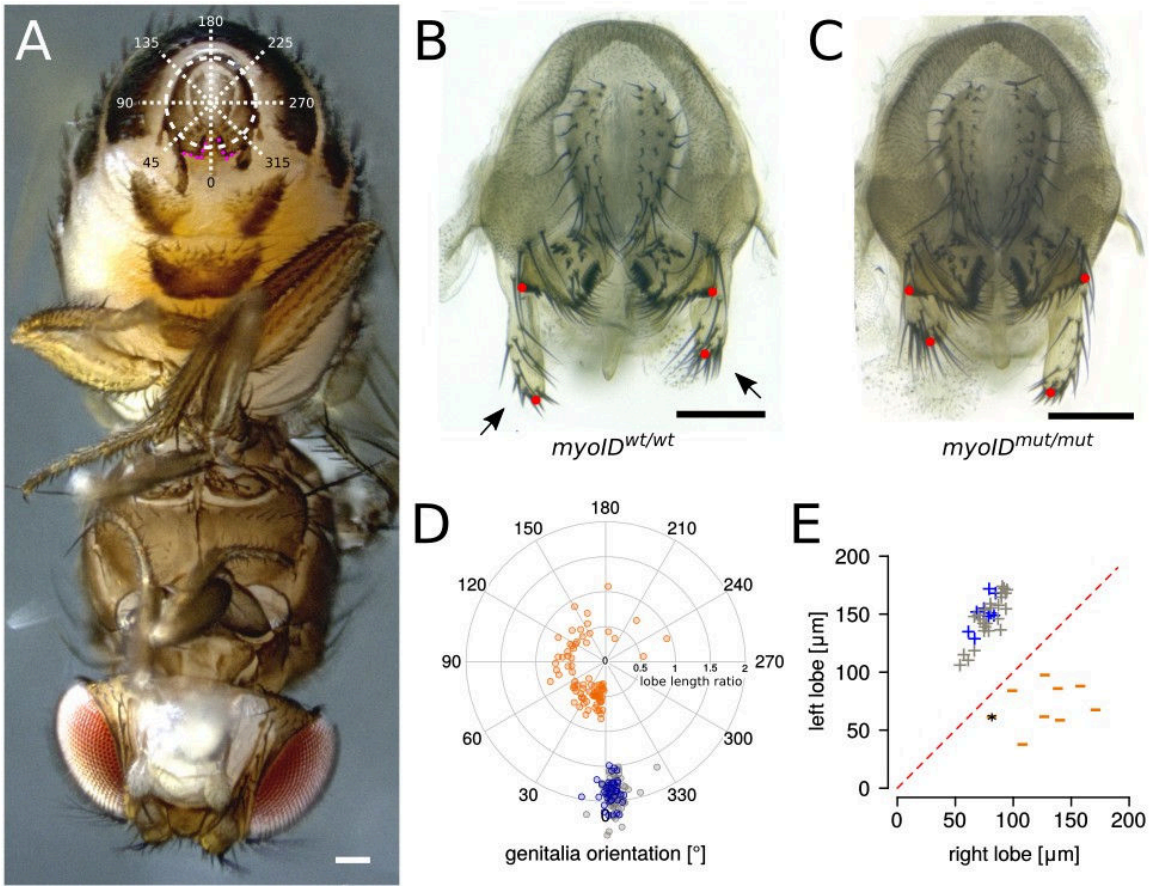


**Fig 1. *MyoID* mutants display reversed genital asymmetry and genitalia rotation defects. (A)** Wild-type *D. pachea* male in ventral view. The orientation of genitalia is measured as an angle between the midpoint of male genital claspers relative to the male midline, as depicted by the dashed polar diagram. Pointed surstili (claspers) are outlined in magenta. The scale is 100 µm. **(B)** External adult male genitalia of a wild-type male *myoID*$^{wt/wt}$ with asymmetric genital lobes at the ventral side (arrows). **(C)** External adult male genitalia of a *myoID*$^{mut/mut}$ mutant male with reversed genital asymmetry. **(B-C)** Lobes are indicated by arrows and lobe length measurement landmarks are shown as red dots. The scale is 100 µm. **(D)** Male genitalia orientation angles and lobe length asymmetry ratio in wild-type *myoID*$^{wt/wt}$ males (blue), heterozygous *myoID*$^{wt/mut}$ mutant males (grey) and homozygous *myoID*$^{mut/mut}$ mutant males (orange). **(E)** The direction of genital lobe asymmetry is associated with the direction of male genitalia rotation. Left and right lobe lengths are plotted for individual males monitored by time-lapse microscopy. Genitalia rotation direction is indicated as +: clockwise, and as -: counter-clockwise. The diagonal red dashed line indicates the 1:1 lobe length ratio. The star indicates an observation with rudimentarily developed lobes in form of buds on both sides.

To monitor genitalia rotation, we inserted a DE-Cadherin::EYFP fusion construct (DE-Cad::EYFP_2) (Material and Methods) into the *myoID*$^{mut/mut}$ stock using piggybac transposon mediated germline transformation (Horn et al.,

2003) (supplementary datafile 2). We examined male genitalia rotation in pupae that were heterozygous for DE-Cad::EYFP to reduce potentially deleterious effects of the piggybac insert (supplementary Figure 3) by time-lapse microscopy (Materials and Methods). We observed that *myoID*$^{wt/wt}$ and *myoID*$^{wt/mut}$ males underwent clockwise genitalia rotation direction (movie 1, n = 9/9, 25/25, respectively), as observed in most schizophoran flies (Feuerborn, 1922; Suzanne et al., 2010) whereas in *myoID*$^{mut/mut}$ males, genitalia rotated counter-clockwise (movie 2, n = 9/9) (Figure 1E, supplementary datafile 1).

**Movie 1.** Clockwise genitalia rotation, acquired by time-lapse microscopy of a *D. pachea* heterozygous *myoID*$^{wt/mut}$ mutant male (supplementary datafile 1, individual 260).

**Movie 2.** Counter-clockwise genitalia rotation, acquired by time-lapse microscopy of a *D. pachea* homozoygous *myoID*$^{mut/mut}$ mutant male (supplementary datafile 1, individual 274).

In 9 monitored males that had developed at least to the pharate adult stage, we were able to dissect male genitalia and to determine the orientation and the lobe length ratio of male genitalia (Figure 1E, supplementary Figure 2). All these *myoID*$^{mut/mut}$ males with counter-clockwise genitalia rotation direction had a reversed lobe length ratio with a longer right lobe and a shorter left lobe, although in one observation lobes were only rudimentarily developed and the measurements were not informative about the lobe length ratio (Figure 1E). In contrast, *myoID*$^{wt/wt}$ and *myoID*$^{wt/mut}$ males had a wild-type lobe ratio. We conclude that in *D. pachea* males MyoID controls genitalia rotation direction, such as previously observed in *D. melanogaster* and that in addition, MyoID determines left-right identity of genitalia.

We investigated if males with reversed genital asymmetry would adopt a reverted copulation posture by monitoring copulation behavior (Figure 2, supplementary datafile 3,4, and 5) of *myoID*$^{wt/wt}$, *myoID*$^{wt/mut}$, or *myoID*$^{mut/mut}$ males with wildtype *myoID*$^{wt/wt}$ females. We annotated the timing of courtship and copulation (supplementary Figure 4, supplementary datafile 4) and in particular we

examined copulation postures (supplementary Figure 5, supplementary datafile 5). A copulation was considered to occur when the male mounted the female and achieved to settle into an invariant copulation position for at least 30 seconds. Alternatively, males were sometimes observed to mount the female, but leg and abdomen movements did not settle and eventually the male separated from the female within a few minutes, which we considered to be a failed mounting attempt (106/140 total attempts, supplementary Figure 4). Only 26% (10/38) of the couples with *myoID*$^{mut/mut}$ males that mounted the female also adopted a stable copulation position, compared to 11/11 and 13/13 for *myoID*$^{wt/wt}$ and *myoID*$^{wt/mut}$ males, respectively. Genitalia orientation angles of *myoID*$^{mut/mut}$ males that managed to adopt a stable copulation posture were found to deviate at most by 16.7° from wild-type orientations, while it was higher in the majority of *myoID*$^{mut/mut}$ males (18/29) that failed to copulate (Figure 1D, supplementary Figure 4). Such defects in genitalia orientation were previously reported to be detrimental for copulation and efficient genitalia coupling for *D. melanogaster myoID* mutants (Inatomi et al., 2019). Regardless of the genotype and direction of genital asymmetry, *myoID*$^{wt/wt}$, *myoID*$^{wt/mut}$ and *myoID*$^{mut/mut}$ males consistently adopted a right-sided average copulation posture (Figure 2). Overall, right-sided mating posture in *D. pachea* does not depend on the direction of male genital asymmetry. Right-sided mating is therefore female-controlled or may be a hard-wired behavior.


7

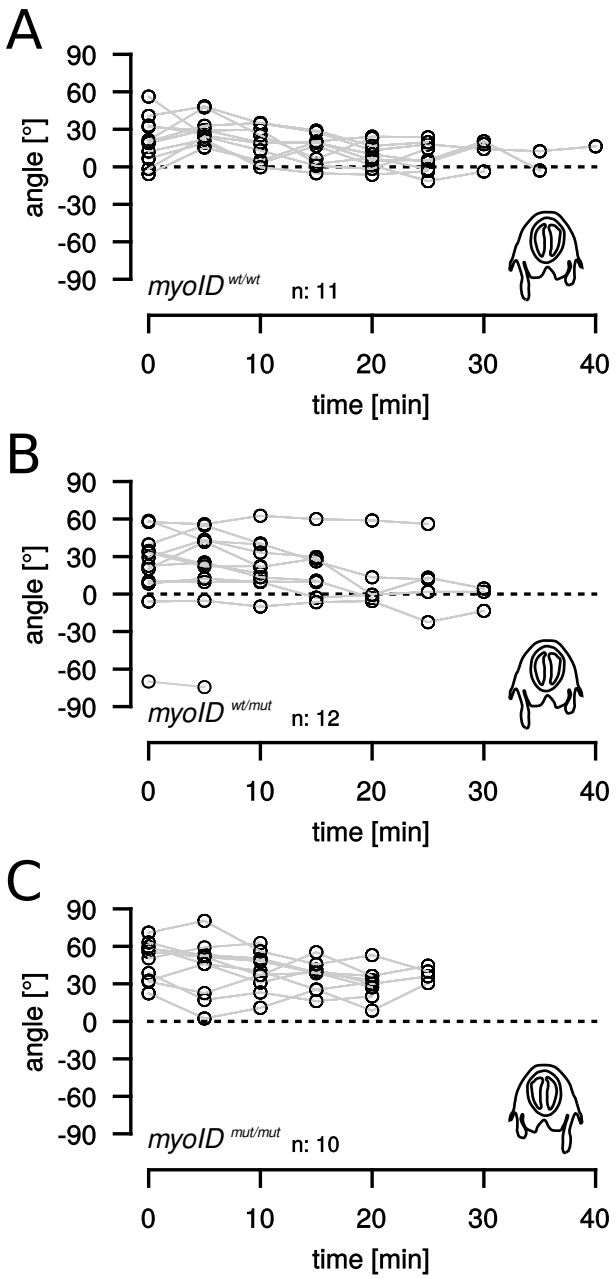


**Fig 2. The right-sided *D. pachea* mating posture does not depend on the direction of male genital asymmetry.** Mating angles (α) (S1 File) of virgin *D. pachea* wild-type females *myoID*$^{wt/wt}$, copulating with a male being either **(A)** *myoID*$^{wt/wt}$ with the wild-type lobe length ratio, **(B)** *myoID*$^{wt/mut}$ heterozygous males with wildtype lobe length ratio, **(C)** *myoID*$^{mut/mut}$ males with reverted lobe asymmetry ratio. The hypothesis angle = 0 was rejected for each male genotype (GLM fit angle ~ genotype, all $p < 1 \times 10^{-10}$). Data acquisition and processing is illustrated in Figure 2 supplements 1 and 2. Positive angle values correspond to right-sided orientations of the male head relative to the female midline. Data points that correspond to the same trial are connected by grey lines. The number of trials are indicated by n, a drawing of the external male genitalia of each genotype is shown on the right.


8

# Ideas and speculation

This study provides the first experimental insights into *de novo* Evolution of left-right asymmetry. It involves recruitment of a conserved left-right regulator and is associated with a pre-existing tissue remodeling process. Our study reveals functional conservation of the unconventional myosin MyoID to control clockwise genitalia rotation in developing *D. pachea* male genitalia. In addition, the same protein got co-opted during evolution of *D. pachea* to contribute to determination of the direction of a novel male genital asymmetry. The latter function may be mediated through the genitalia rotation process itself since rotation direction and genital asymmetry direction are perfectly associated in our live-imaging trials. Changes in mechanical cell or tissue interactions may be cues for morphological diversification. The rotation direction can potentially be translated into morphological asymmetry through direct mechanical interactions of the rotating and non-rotating tissue, for example via friction forces that are supposed to act in opposite direction at the left and the right side of the genitalia. Indeed, live-imaging of rotating genitalia reveals an intermediate accumulation of a tissue bud in the close sourrounding of rotating genitalia primordia, approximately between 90° and 180° of rotation when lobe asymmetry becomes apparent (supplementary Figure 6), indicating tissue tensions. In *myoID*$^{mut/mut}$ males, a similar bud is observed in a similar orientation but appears during the second half of rotation, between 180° and 270° (supplementary Figure 7). This indicates that a potential mechanical interaction of the left ventral ventral abdomen with developing genital lobes does not rely on MyoID function itself and that is not reversed in *myoID*$^{mut/mut}$ males. A similar finding that external components affect genitalia evolution was reported in *Drosophila melanogaster* and closely related species, where interspecific shape variation of male genital posterior lobes were shown to depend on mechanical interactions of genital tissue and the covering extracellular matrix, resulting in a tinkering of cell size and shapes (Smith et al., 2020).

Alternatively, rotation direction may translate a dorso-ventral gradient of signaling factors into left-right information. For example, the rotation direction may bring


9

the left lobe earlier into contact with a growth promoting factor than the right lobe. Changing the sense of rotation direction reverse asymmetry by reverting the timing of exposition of left and right sides of genitalia. One way or another, evolution of morphological asymmetry appears to involve complex tissue interactions and remodeling of the entire genital primordia.

Male genital asymmetry does not determine the lateralized *D. pachea* mating posture since wildtype and mutant males with reversed genital asymmetry consistently mate in a right-sided copulation posture. Right-sided mating is therefore female-controlled or may be a behavior hard-wired in males. This posture could have possibly favored the evolution of morphological asymmetry as an instructive cue to optimize genital contacts and sperm transfer (Huber, 2010). Future studies should focus on the expression and distribution of mechanoreceptors in male genitalia that may guide the positioning of the male onto the female. In addition, the female uterus may twist the intermittent male phallus. It is known that the female reproductive tract rearranges during copulation (Mattei et al., 2015; van Gammeren et al., 2022) and the dynamic uterus contractions should be monitored during copulation to further understand their potential role in directing mating posture and their interaction with genital morpology.

# Materials and Methods

### Generation of MyoID mutants

The *D. pachea myoID* ortholog was identified by sequence comparisons of *D. melanogaster myoID* cDNA sequence NM_001201855.2 and the *D. pachea* genome assembly JABVZX000000000 (Suvorov et al., 2021) (supplementary Figure 1). CRISPR targets were searched manually and single guide RNA synthesis was performed *in vitro* according to (Bassett et al., 2013) (supplementary datafile 6). The sgRNA/Cas-9 complexes were injected using standard Drosophila germline transformation procedures (see detailed protocol). The injection mix contained 0.1 µg/µL sgRNA, 2 µM NLS-Cas9 (New England Biolabs) and 1x NLS-Cas9 reaction Buffer (New England Biolabs).


10

Emerging adults from injections were crossed to non-injected individuals and resulting progeny was maintained for several generations. Candidate stocks for CRISPR mutants were identified by visual inspection of male adults that had genitalia rotation defects. Candidate stocks were screened for *myoID* mutations by PCR and Sanger sequencing (supplementary datafile 1). We identified a mutation at position 1724 downstream of the translation start codon, which contained a 13-bp deletion and a 7-bp insertion (supplementary Figure 1). The frameshift leads to a premature stop codon, abolishing 443 native codons that encode the C-terminal part of MyoID (supplementary Figure 1 B,C, supplementary datafile 1). The identified mutation also contained a *Nco*I restriction site (supplementary Figure 1 B), not present in the wild-type allele. We took advantage of this restriction site to determine the genotype of *D. pachea* individuals (Figure supplement 1 D, supplementary datafile 1). Prior to genotyping, genitalia of male adults or pupae were dissected and imaged (supplementary Figure 2, supplementary datafile 1).

**Generation act5C::DE-Cad-EYFP_2 flies**

We generated a membrane specific EYFP cellular marker pB-act5C::DE-Cad-EYFP that contains a partial *D. melanogaster* DE-Cadherin (*shg*) and EYFP coding sequences (supplementary datafile 1). The assembled gene construct includes the *D. melanogaster shg* 5'UTR and two initial cadherin repeats, the DE-cadherin trans-membrane domain and a part of the cytoplasmic domain without the β-Catenin binding domain. The gene construct was inserted into the vector backbone of pBAC-ECFP-15xQUAS_TATA-mcd8-GFP-SV40 (Addgene 104878) and the 3xP3 ECFP integration reporter was replaced by 3xP3 DsRed (Matz et al., 1999). transgenic flies were produced by germline transformation as described above. Identification of act5C::DE-Cad-EYFP_2 transgenic flies was achieved by evaluation of eye fluorescence driven by the 3xP3 DsRed integration reporter. The insertion site was mapped to position 14,614,126 on contig tig00000094 (supplementary datafile 1), inside the first 31.95-kb intron of the putative *D. pachea wheeler18* gene homolog.


11

### Genitalia live imaging

We followed a particular crossing scheme to analyze genitalia rotation of varying *myoID* genotypes in a heterozygous act5C::DE-Cad-EYFP_2 background (supplementary Figure 3). Time-lapse microscopy of developing genitalia was performed at 20 – 25 h after the puparium had formed on a DMI8 inverted microscope (Leica), equipped with a spinning-disc head CSU-W1 (Yokogawa Corporation of America) and controlled by MetaMorph software (Molecular Devices). Imaging up to 20 samples in parallel was carried out at 200 fold magnification for 15 -24 h, by acquisition of individual z-stacks every 30 min (Source datafie 1 File).

### Evaluation of mating behavior

We performed video-recording of virgin but sexually mature *D. pachea* individuals (Figure 2 supplements 1 and 2, supplementary datafiles 3 and 4), also described in (Acurio et al., 2019) and (Lefèvre et al., 2021). Mating position analysis (supplementary Figure 5, supplementary datafile 5) was carried out as described in (Acurio et al., 2019).

## Data availability

Data supporting this article is available as supplementary datafiles and raw data has been deposited at the DRYAD database (doi:10.5061/dryad.bzkh189bd), except for DNA sequence data of the *D. pachea myoID* coding sequence, which was deposited at NCBI (accession number OM240650).

## Acknowledgments

We thank Stéphane Prigent for preparation of Drosophila genitalia. We acknowledge the ImagoSeine core facility of the Institut Jacques Monod, member of IBiSA and France-BioImaging (ANR-10-INBS-04) infrastructures for assistance in microscopy. We are grateful to Nicolas Gompel for initial help with *Drosophila* germline transfection and to Carolina Parada for comments on the manuscript.


12

# References


Acurio A, Rhebergen FT, Paulus SE, Courtier-Orgogozo V, Lang M. 2019. Repeated evolution of asymmetric genitalia and right-sided mating behavior in the *Drosophila nannoptera* species group. *BMC Evolutionary Biology* **19**:109. doi:10.1186/s12862-019-1434-z

Bassett AR, Tibbit C, Ponting CP, Liu J-L. 2013. Highly Efficient Targeted Mutagenesis of *Drosophila* with the CRISPR/Cas9 System. *Cell Reports* **4**:220–228. doi:10.1016/j.celrep.2013.06.020

Benitez S, Sosa C, Tomasini N, Macias A. 2010. Both JNK and apoptosis pathways regulate growth and terminalia rotation during *Drosophila* genital disc development. *Int J Dev Biol* **54**:643–653.

Chougule A, Lapraz F, Földi I, Cerezo D, Mihály J, Noselli S. 2020. The *Drosophila* actin nucleator DAAM is essential for left-right asymmetry. *PLOS Genetics* **16**:e1008758.

Feuerborn HJ. 1922. Das Hypopygium 'inversum' und 'circumversum' der Dipteren. *Zoologischer Anzeiger* **55**:89–213.

González-Morales N, Géminard C, Lebreton G, Cerezo D, Coutelis J-B, Noselli S. 2015. The Atypical Cadherin Dachsous Controls Left-Right Asymmetry in *Drosophila*. *Developmental Cell* **33**:675–689. doi:10.1016/j.devcel.2015.04.026

Hamada H, Tam P. 2020. Diversity of left-right symmetry breaking strategy in animals. *F1000Research* **9**:F1000 Faculty Rev-123. doi:10.12688/f1000research.21670.1

Hatori R, Ando T, Sasamura T, Nakazawa N, Nakamura M, Taniguchi K, Hozumi S, Kikuta J, Ishii M, Matsuno K. 2014. Left–right asymmetry is formed in individual cells by intrinsic cell chirality. *Mechanisms of Development* **133**:146–162. doi:https://doi.org/10.1016/j.mod.2014.04.002

Horn C, Offen N, Nystedt S, Häcker U, Wimmer EA. 2003. piggyBac-Based Insertional Mutagenesis and Enhancer Detection as a Tool for Functional Insect Genomics. *Genetics* **163**:647 LP – 661.

Hozumi S, Maeda R, Taniguchi K, Kanai M, Shirakabe S, Sasamura T, Spéder P, Noselli S, Aigaki T, Murakami R, Matsuno K. 2006. An unconventional myosin in *Drosophila* reverses the default handedness in visceral organs. *Nature* **440**:798–802. doi:10.1038/nature04625

Huber BA. 2010. Mating positions and the evolution of asymmetric insect genitalia. *Genetica* **138**:19–25.

Inatomi M, Shin D, Lai Y-T, Matsuno K. 2019. Proper direction of male genitalia is prerequisite for copulation in *Drosophila*, implying cooperative evolution between genitalia rotation and mating behavior. *Scientific Reports* **9**:210. doi:10.1038/s41598-018-36301-7

Jinek M, Chylinski K, Fonfara I, Hauer M, Doudna JA, Charpentier E. 2012. A Programmable Dual-RNA–Guided DNA Endonuclease in Adaptive Bacterial Immunity. *Science* **337**:816–821. doi:10.1126/science.1225829

Juan T, Géminard C, Coutelis J-B, Cerezo D, Polès S, Noselli S, Fürthauer M. 2018. Myosin1D is an evolutionarily conserved regulator of animal left–right asymmetry. *Nature Communications* **9**:1942. doi:10.1038/s41467-018-04284-8

Lai Y-T, Takeshi S, Kuroda J, Maeda R, Nakamura M, Hatori R, Ishibashi T, Taniguchi K, Ooike M, Taguchi T, Nakazawa N, Hozumi S, Okumura T, Aigaki T, Inaki M, Matsuno K. 2022. The Drosophila AWP1 ortholog Doctor No regulates JAK/STAT signaling for left-right asymmetry in the gut by promoting receptor endocytosis. *bioRxiv* 2022.08.20.504629. doi:10.1101/2022.08.20.504629

Lang M, Orgogozo V. 2012. Distinct copulation positions in *Drosophila pachea* males with symmetric or asymmetric: External genitalia. *Contributions to Zoology* **81**:87–94.



13

Lang M, Polihronakis Richmond M, Acurio AE, Markow TA, Orgogozo V. 2014. Radiation of the *Drosophila nannoptera* species group in Mexico. *Journal of Evolutionary Biology* **27**:575–584. doi:10.1111/jeb.12325

Lebreton G, Géminard C, Lapraz F, Pyrpassopoulos S, Cerezo D, Spéder P, Ostap E M, Noselli S. 2018. Molecular to organismal chirality is induced by the conserved myosin 1D. *Science* **362**:949–952. doi:10.1126/science.aat8642

Lefèvre BM, Catté D, Courtier-Orgogozo V, Lang M. 2021. Male genital lobe morphology affects the chance to copulate in *Drosophila pachea*. *BMC Ecology and Evolution* **21**:23. doi:10.1186/s12862-021-01759-z

Macias A, Romero NM, Martin F, Suarez L, Rosa AL, Morata G. 2004. PVF1/PVR signaling and apoptosis promotes the rotation and dorsal closure of the *Drosophila* male terminalia. *Int J Dev Biol* **48**:1087–1094.

Mattei AL, Riccio ML, Avila FW, Wolfner MF. 2015. Integrated 3D view of postmating responses by the *Drosophila melanogaster* female reproductive tract, obtained by micro-computed tomography scanning. *Proc Natl Acad Sci U S A* **112**. doi:10.1073/pnas.1505797112

Matz M V, Fradkov AF, Labas YA, Savitsky AP, Zaraisky AG, Markelov ML, Lukyanov SA. 1999. Fluorescent proteins from nonbioluminescent Anthozoa species. *Nature Biotechnology* **17**:969–973. doi:10.1038/13657

Okumura T, Sasamura T, Inatomi M, Hozumi S, Nakamura M, Hatori R, Taniguchi K, Nakazawa N, Suzuki E, Maeda R, Yamakawa T, Matsuno K. 2015. Class I Myosins Have Overlapping and Specialized Functions in Left-Right Asymmetric Development in *Drosophila*. *Genetics* **199**:1183–1199. doi:10.1534/genetics.115.174698

Petzoldt AG, Coutelis J-B, Géminard C, Spéder P, Suzanne M, Cerezo D, Noselli S. 2012. DE-Cadherin regulates unconventional Myosin ID and Myosin IC in *Drosophila* left-right asymmetry establishment. *Development* **139**:1874–1884. doi:10.1242/dev.047589

Pitnick S, Heed W. 1994. New Species of Cactus-Breeding *Drosophila* (Diptera: Drosophilidae) in the Nannoptera Species Group. *Annals of the Entomological Society of America* **87**:307–310.

Rhebergen FT, Courtier-Orgogozo V, Dumont J, Schilthuizen M, Lang M. 2016. *Drosophila pachea* asymmetric lobes are part of a grasping device and stabilize one-sided mating. *BMC Evolutionary Biology* **16**:176. doi:10.1186/s12862-016-0747-4

Rousset R, Bono-Lauriol S, Gettings M, Suzanne M, Spéder P, Noselli S. 2010. The *Drosophila* serine protease homologue Scarface regulates JNK signalling in a negative-feedback loop during epithelial morphogenesis. *Development* **137**:2177–2186. doi:10.1242/dev.050781

Smith SJ, Davidson LA, Rebeiz M. 2020. Evolutionary expansion of apical extracellular matrix is required for the elongation of cells in a novel structure. *eLife* **9**:e55965. doi:10.7554/eLife.55965

Spéder P, Ádám G, Noselli S. 2006. Type ID unconventional myosin controls left–right asymmetry in *Drosophila*. *Nature* **440**:803–807. doi:10.1038/nature04623

Suvorov A, Kim BY, Wang J, Armstrong EE, Peede D, D'Agostino ERR, Price DK, Wadell P, Lang M, Courtier-Orgogozo V, David JR, Petrov D, Matute DR, Schrider DR, Comeault AA. 2021. Widespread introgression across a phylogeny of 155 *Drosophila* genomes. *Current Biology* **32**:111–123. doi:10.1101/2020.12.14.422758

Suzanne M, Petzoldt AG, Spéder P, Coutelis J-B, Steller H, Noselli S. 2010. Coupling of Apoptosis and L/R Patterning Controls Stepwise Organ Looping. *Current Biology* **20**:1773–1778. doi:doi: 10.1016/j.cub.2010.08.056

Taniguchi K, Hozumi S, Maeda R, Ooike M, Sasamura T, Aigaki T, Matsuno K. 2007. D-JNK signaling in visceral muscle cells controls the laterality of the *Drosophila* gut. *Developmental Biology* **311**:251–263. doi:https://doi.org/10.1016/j.ydbio.2007.08.048


14

Taniguchi K, Maeda R, Ando T, Okumura T, Nakazawa N, Hatori R, Nakamura M, Hozumi S, Fujiwara H, Matsuno K. 2011. Chirality in Planar Cell Shape Contributes to Left-Right Asymmetric Epithelial Morphogenesis. *Science* **333**:339–341. doi:10.1126/science.1200940

Tingler M, Kurz S, Maerker M, Ott T, Fuhl F, Schweickert A, LeBlanc-Straceski JM, Noselli S, Blum M. 2018. A Conserved Role of the Unconventional Myosin 1d in Laterality Determination. *Current Biology* **28**:810-816.e3. doi:10.1016/j.cub.2018.01.075

van Gammeren S, Ruecklin M, Lang M, Schilthuizen M. 2022. No evidence for asymmetric sperm deposition in a species with asymmetric male genitalia. *PeerJ* **10**:e14225 https://doi.org/10.7717/peerj.14225



15

# supplementary Figures

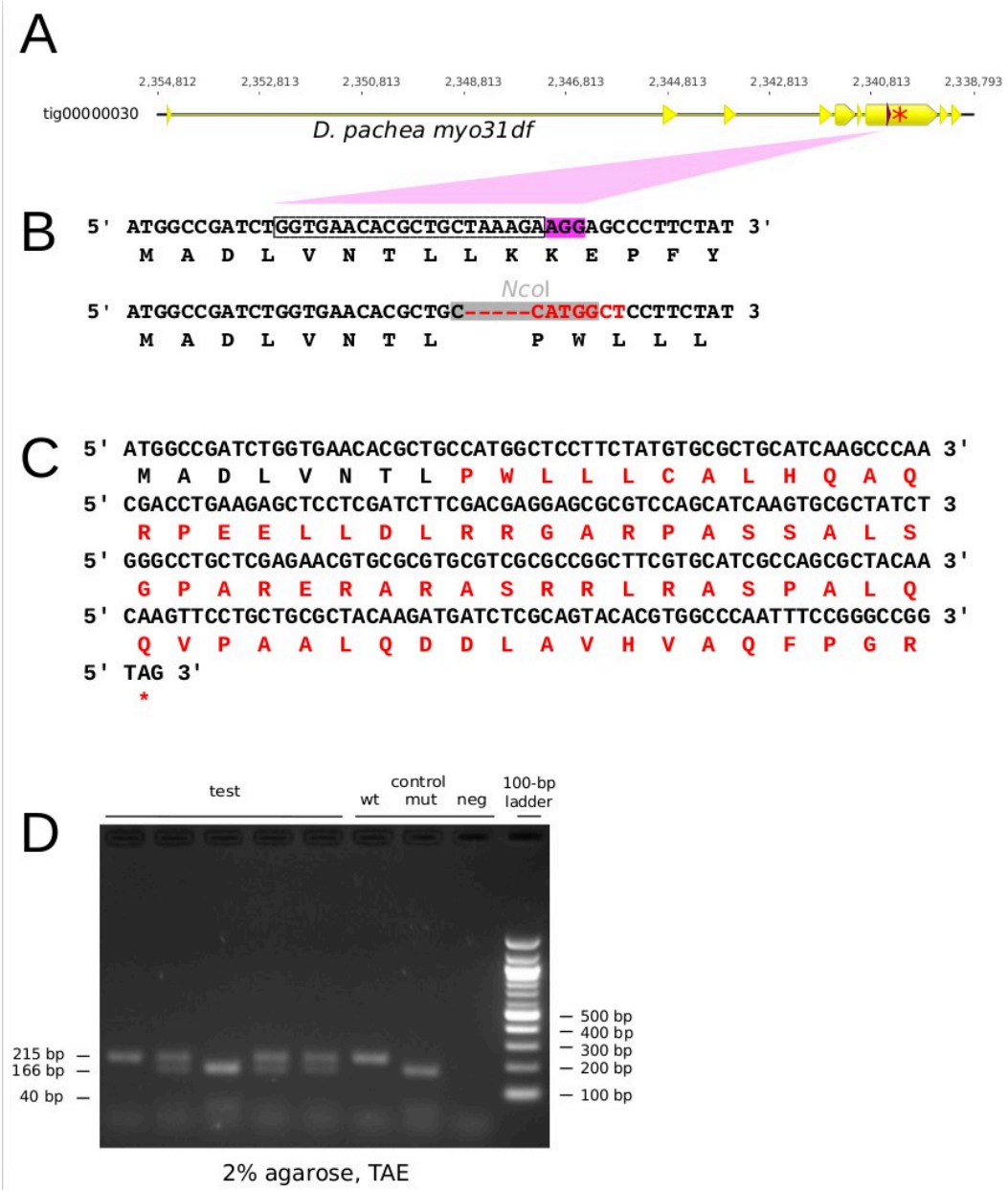


**supplementary Figure 1. Identification of the myoID mutation. (A)** Annotation of the *myoID* coding sequence (orange). Orange arrows indicate coding exons, numbers indicate the nucleotide positions relative to contig tig00000030, the violet arrow indicates the CRISPR target site and the red star indicates the location of the premature stop codon in the myoID mutant. **(B)** Nucleotide and amino acid sequences at the CRISPR target site. The upper line corresponds to the *D. pachea* wild-type *myoID* sequence, the lower line to the CRISPR/Cas-9 induced frameshift mutation. Outlined framed positions indicate the single guide RNA (sgRNA) sequence to target *myoID*, dark-violet highlights the protospacer adjacent motif (PAM). The mutated positions are in red, the *Nco*I endonuclease motif is highlighted in grey. Single letter amino acid abbreviations are presented beneath each codon. **(C)** The mutation causes a frameshift. Altered amino acid


16

sequence is indicated by red single letter amino acid abbreviations, **(D)** Gel electrophoresis of *Nco*I digested PCR products, used to distinguish *D. pachea* male genotypes. Test indicates lanes corresponding to genomic DNA of males 6U, 8A, 8C, 8D and 8E (supplementary datafile 2), used for time-lapse microscopy. Controls indicate a *myoID*$^{+/+}$ male (wt), a *myoID*$^{-/-}$ male (mut) and a negative control amplified from water (neg). The 100 bp ladder is presented on the right. Relevant DNA fragment sizes are indicated at the sides of the image, the agarose concentration and gel electrophoresis buffer is annotated below the image.

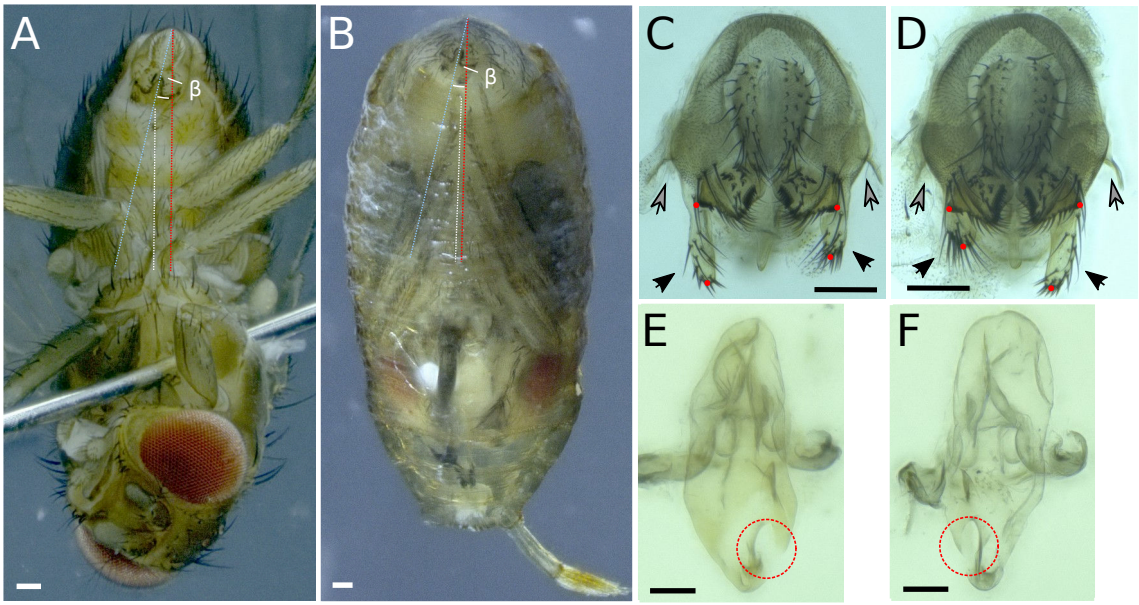


**supplementary Figure 2. Quantification of genitalia morphology. (A)** Male genitalia orientation was measured as the angle (β) between the dorso-ventral axis of male genitalia (blue dashed line) relative to the male antero-posterior body axis (white and red dashed lines). **(B)** genitalia orientation was also measured in male pupae where genitalia were visible. The midline was approximated as a medial line between the ventrally located legs (white dashed line). **(C-D)** The length of the lobes (black arrows) in wildtype genitalia **(C)**, heterozygous *myoID*$^{wt/mut}$ mutants, and homozygous *myoID*$^{mut/mut}$ mutants **(D)** was measured as the distance between the pointed outer edge of the surstili (upper red points) and the medial tip of each lobe (lower red points). The lateral spine is indicated by grey arrows. **(A-D)** The scale is 100 µm. **(E-F)** Phallus of a *myoID*$^{wt/mut}$ male **(E)** and *myoID*$^{mut/mut}$ male **(F)** with the gonopore (highlighted by red dashed circles) on the right and left side, respectively. The scale is 50 µm.


17

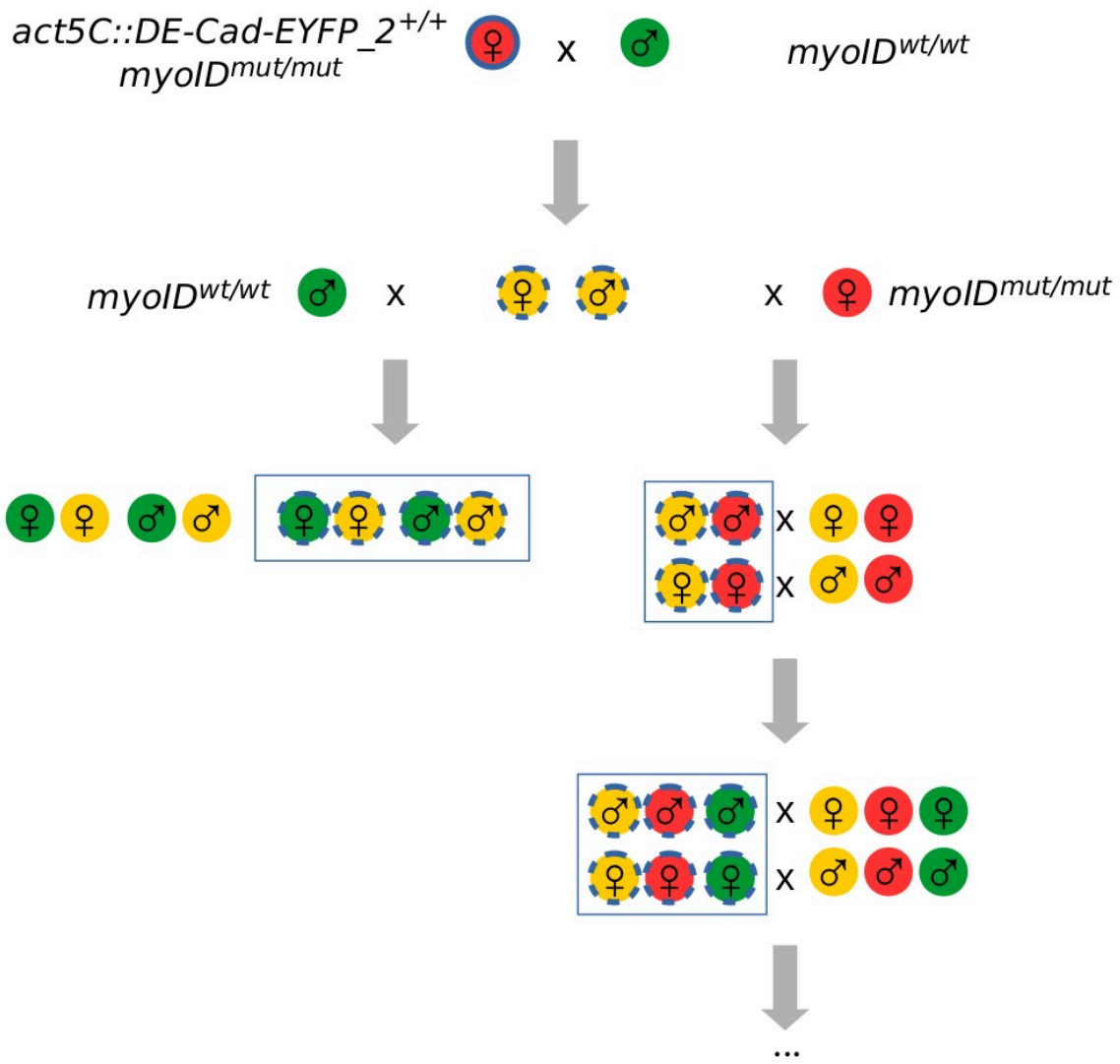


**supplementary Figure 3. Crossing scheme for time-lapse microscopy samples.** Homozygous females [*myoID*$^{mut/mut}$, act5C::DE-Cad-EYFP_2$^{+/+}$] were crossed to wild-type males [*myoID*$^{wt/wt}$, act5C::DE-Cad-EYFP_2$^{-/-}$]. The female F1 progeny was crossed back to wild-type males and male progeny was crossed to *myoID* homozygous mutant males [*myoID*$^{mut/mut}$, act5C::DE-Cad-EYFP_2$^{-/-}$]. The progeny of the latter cross was then maintained by sibling crosses: females [act5C::DE-Cad-EYFP_2$^{+/-}$] with males [act5C::DE-Cad-EYFP_2$^{-/-}$] and females [act5C::DE-Cad-EYFP_2$^{-/-}$] with males [act5C::DE-Cad-EYFP_2$^{+/-}$]. The presence of the act5C::DE-Cad-EYFP_2 insertion was visible under a fluorescence stereomicroscope by the presence of red fluorescence in the adult eyes. Colored circles indicate *myoID* genotypes, green: *myoID*$^{wt/wt}$, yellow: *myoID*$^{wt/mut}$, red: *myoID*$^{mut/mut}$. Outlines indicate act5C::DE-Cad-EYFP_2 insertion, absent: no insertion, dashed: heterozygous insertion/no insertion, full: homozygous for the insertion. Open squares indicates genotypes of individuals used for time-lapse imaging. Times-lapse imaging was performed on individuals originating from the first three successive generations.


18

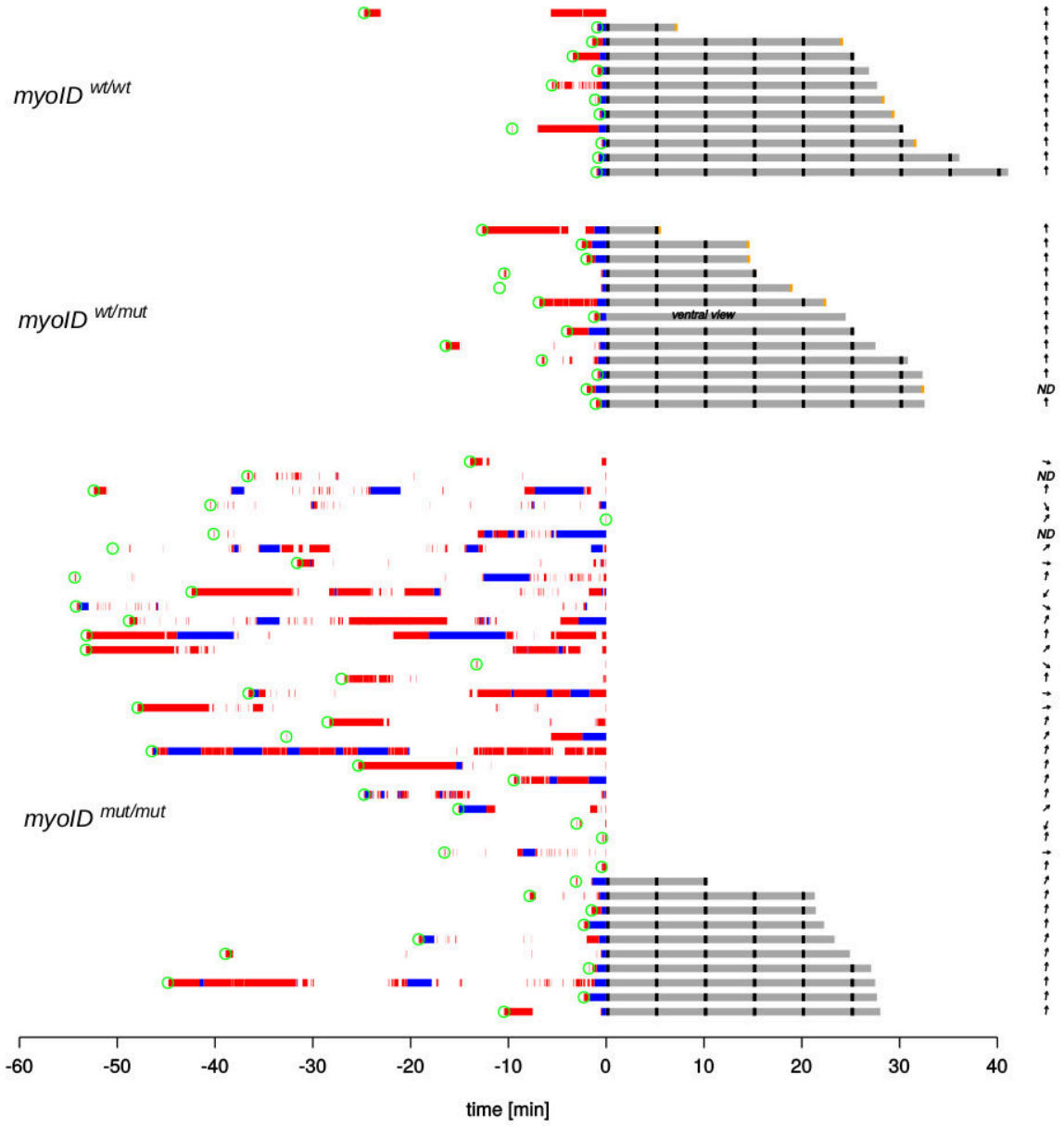


**supplementary Figure 4. Mating behavior of *D. pachea* males differing in *myoID* genotype.** This ethogram summarizes mating behavior observations (supplementary datafile 4) of copulation recording trials (supplementary datafile 3). Each line presents one mating trial and trials are grouped by male *myoID* genotype. Green circles indicate courtship start, red segments indicate male licking behavior, blue segments mounting attempts, grey segments stable copulation, overlaid by black tick marks that indicate moments of mating position measurements (supplementary datafile 5). In one trial copulation is labeled "ventral view" because the copulation was observed in ventral view so that position landmarks (supplementary Figure 5) could not be determined. The arrow on the right indicates the orientation of male genitalia (Figure 1, supplementary datafile 1) with 0° on top. ND indicates non determined genitalia orientation angles.


19

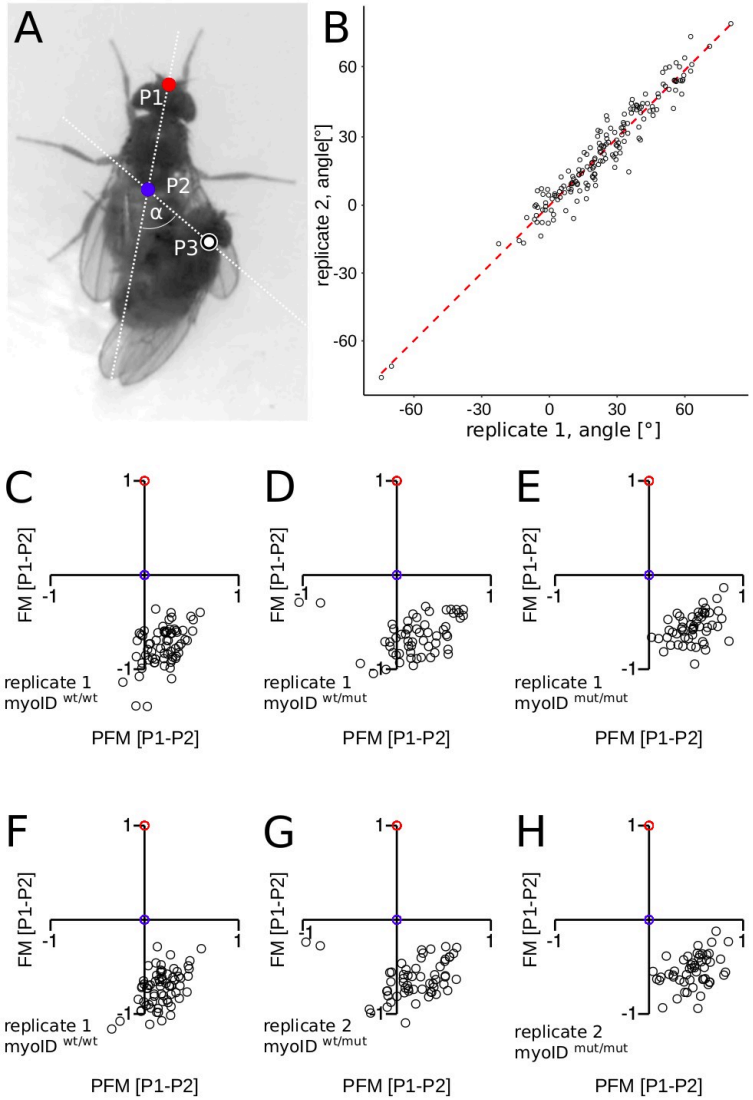


**supplementary Figure 5. Quantification of copulation postures. (A)** Landmarks to approximate the male head position relative to the female midline as described in (Acurio et al., 2019): P1 (red point) is the anterior medial tip of the female head, P2 (blue point) the distal tip of the female scutellum and P3 (white open circle) is the most posterior medial point of the male head (supplementary datafile 5). The angle (α) between white lines (P1-P2) and (P2-P3) was used to measure sidedness of the mating position on each extracted image. **(B)** Scatter plot of mating angles obtained from two replicate analyses from two persons, Pearson correlation ($t = 50.193$, $df = 175$, $p < 2.2 \times 10^{-16}$, $r = 0.9669795$). The red dashed line corresponds to the linear regression line. Variation in angle estimates was found to be attributable mostly to individual images of the different movies (image) but not to replicate measurements (replicate) (ANOVA, angle ~ image + replicate, image: $df1 = 176$, $df2 = 1$, image: $F = 58.74$, $p < 10^{-16}$, replicate: $F = 0.148$, $p = 0.701$). **(C-H)** landmark positions of each analysis and genotype, rotated and scaled relative to the distance P1-P2. All P2 points were super-imposed onto the diagram origin and P1 points were aligned onto position (0,1). The FM axis corresponds to the female midline, PFM axis is perpendicular to the female midline.


20

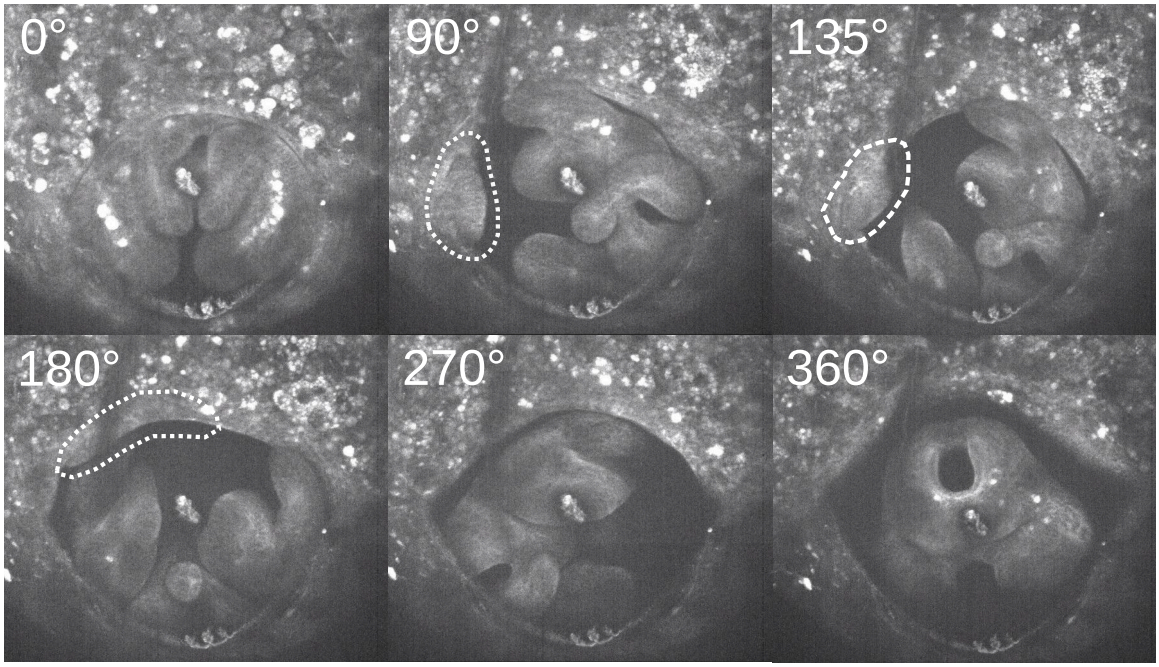


**supplementary Figure 6. Genitalia rotation involves surrounding tissue agglomeration.** Snapshots from movie 1, time-lapse microscopy of a *D. pachea* heterozygous *myoID*$^{wt/mut}$ mutant male (supplementary datafile 1, individual 260). The rotation angle relative to rotation start positioning of genitalia is indicated on each panel. Tissue agglomeration is outlined with a white, dashed line.

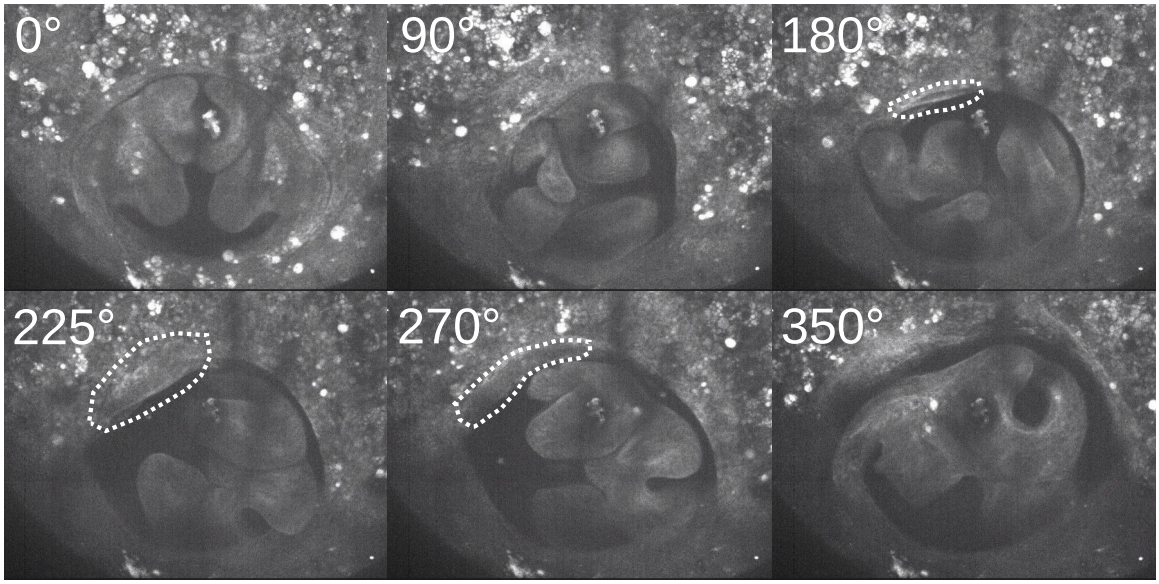


**supplementary Figure 7. Tissue agglomeration during genitalia rotation in a MyoID mutant male.** Snapshots from movie 2, time-lapse microscopy of a *D. pachea* homozygous *myoID*$^{mut/mut}$ mutant male (supplementary datafile 1, individual 274). The rotation angle relative to rotation start positioning of genitalia is indicated on each panel. Tissue agglomeration is outlined with a white, dashed line.


21

**supplementary datafile 1** Male *D. pachea* genitalia morphology and orientation, spreadsheet with length and orientation measurements of genital morphology of male *D. pachea* flies.

**supplementary datafile 2** Time-lapse microscopy trials, summary of trials and conditions for time-lapse microscopy.

**supplementary datafile 3** Single couple mating trials, summary of *D. pachea* single couple mating trials.

**supplementary datafile 4** Courtship and copulation behavior, annotated courtship and copulation behavior. The data is summarized in supplementary Figure 4.

**supplementary datafile 5** Copulation position coordinates, position landmarks to compare copulation postures. The data is the main input file for Figure 2.

**supplementary datafile 6**. Oligonucleotides for PCR and preparation of CRISPR sgRNA. Tan °C: annealing temperatures used in our experiments. *: touch-down annealing temperature


22